

# HIGH SURFACE AREA GRAPHITE NANOPARTICLES FROM NATURAL GRAPHITE FLAKES AND EXFOLIATED GRAPHITE NANOPATELETS

I.H. Do, W. Liu, and L.T. Drzal  
Composite Materials and Structures Center, Michigan State University,  
East Lansing, MI 48824, USA  
doinhwan@egr.msu.edu

## SUMMARY

High surface area graphite nanoparticles (HSAG) were fabricated via a high energy ball milling process from natural graphite flake (NG) and exfoliated graphite nanoplatelets (xGnP). The as-produced HSAG was characterized for its surface and physical properties by using various methods. HSAG-reinforced polymeric composites were fabricated and their mechanical and electrical properties were investigated.

*Keywords: exfoliated graphite nanoplatelets, natural graphite flakes, high surface area graphite, high energy ball milling, polymeric composites*

## INTRODUCTION

Graphitic nanomaterials possess excellent mechanical, thermal, and electrical properties, high surface area, excellent dimensional stability, and excellent optical properties [1]. Hence they have attracted great attention due to their promising potential for wide applications such as transistor, battery, supercapacitor, fuel cell, biosensor, composites, and so on [2~5]. Recent work at our group has shown that it is possible to develop multifunctional polymer-xGnP nanocomposites which can be suitable for the applications requiring enhanced mechanical properties and electrical and thermal conductivity. xGnP-reinforced epoxy nanocomposites have been fabricated and showed excellent electrical and thermal properties and much better mechanical properties than the nanocomposites reinforced with carbon black and vapour grown carbon fiber [6]. xGnP-reinforced vinyl ester (VE) nanocomposites have also been prepared [7]. The mechanical strength and electrical resistivity of xGnP-reinforced VE nanocomposites depended strongly on the aspect ratio of xGnP. In addition, it has been shown that it is possible to optimize mechanical, thermal, and electrical properties of VE nanocomposites by combining different sizes of xGnP.

Mechanical milling has been known to be an effective way to prepare nanocrystalline structures and thus used to produce high surface area graphite (HSAG). HSAG produced via a mechanical milling process can show much better performance as catalyst supports and adsorbents than conventional activated carbons and also be promising reinforcing materials for polymeric nanocomposites due to the presence of oxygen containing functional groups resulting from high energy milling process [8~10].

The purpose of the present work is to produce HSAG via high energy ball milling, to characterize their fundamental properties such as morphology, structural information, surface area, thermal behavior of HSAG and to investigate the reinforcing effect of HSAG on polymeric nanocomposites.

## EXPERIMENTAL

### Materials

Commercial Graflake 99550PO (4g) (> 99% in purity and > 300 $\mu$ m in average size) or xGnP (3g) obtained by exfoliating acid-intercalated graphite was milled in High-energy SPEX 8000D shake mixer/mill equipped with hardened steel vials containing 6 stainless steel balls (SS balls, 2 of 1/2" and 4 of 1/4" in diameter) and polypropylene (PP balls, 1/4" in diameter). The surface area of the HSAG was altered by changing the milling time. The as-produced HSAG from NG and xGnP are identified HSANG-X and HSAGxGnP-X in which X represents surface area. All of the produced HSAG was degassed in a vacuum oven for a day to remove any trapped gas. xGnP-1 (1 $\mu$ m average diameter), xGnP-15 (15 $\mu$ m average diameter), multi-walled carbon nanotube (MWNT, Nanocyl™ NC3100), and single walled carbon nanotube (SWNT, 90% specification grade of Cheaptubes Inc.) were used to compare their performance. Vinyl ester resin 411-350 was supplied by Ashland Specialty Chemical, Division of Ashland INC (Columbus, OH). Butanone peroxide, N,N-Dimethylaniline, cobalt naphthenate, and 2,4-Pentanedione were obtained from Aldrich.

### Nanocomposite Preparation

Mixing of the vinyl ester 411-350 resin solution with 1wt.% of xGnP was conducted in a glass beaker under mechanical stirring for approximately 24 hours. Then, the mixture of xGnP and vinyl ester was continuously sonicated with 100W output for less than 30 min. 1% of butanone peroxide, 0.1% of 2,4-pentanedione, 0.1% of N,N-dimethylaniline, and 0.2% of cobalt naphthenate were added to the mixed vinyl ester resin solution in order and mixed for 10 min. The above mixed resin solution was poured into a 6'x6'x0.125' plaque mold, which was mounted on a vibration plate to accelerate the viscous resin flow to the bottom of the mold. Finally, resin solution was cured at 80°C for 3 hours and post-cured at 120°C for 2 hours. Coupons for testing of the cured xGnP and HSAG-reinforced VE nanocomposites were cut with a diamond saw to obtain specimens to measure the mechanical and electrical properties.

### Characterization of HSAG

The surface morphology of HSAG was examined with a scanning electron microscope (JEOL 6400V) operated at 15kV and a transmission electron microscope (JEOL CX100) operated at 100kV. The specific surface area was determined from N<sub>2</sub> adsorption isotherm at 77K (Micromeritics ASAP 2020) by using Brunauer-Emmett-Teller (BET) theory. Thermo-gravimetric Analysis (TGA 2950, TA instrument) was performed over temperatures ranging from room temperature to 1000°C at 10°C/min under an air environment to determine the thermal stability of HSAG. X-ray diffraction

(XRD) patterns were collected on a Regaku Rotaflex 200B X-ray diffractometer using  $\text{Cu-K}_\alpha$  radiation with a curved graphite monochromator. The samples were scanned in  $2\theta$  region between  $10^\circ$  and  $100^\circ$  at 45 keV and 100 mV at a scan rate of  $5^\circ/\text{min}$ . The flexural properties of the reinforced VE nanocomposites were measured with a United Testing System SFM-20 according to ASTM D790. System control and data analysis were performed using Datum software. The notched Izod impact strength was measured with a Testing Machines Inc. 43-02-01 Monitor/Impact machine according to ASTM D256. The electrical resistivity of the nanocomposites was calculated from the AC impedance spectra over a range of frequencies with a Gamry instrument under FAS2 Femtostat plug system and potentiostatic mode.

## RESULTS AND DISCUSSION

### Fundamental Properties of Milled Graphite

The specific surface area (SSA) of HSAG produced from natural graphite (NG) and xGnP as a function of milling time is shown in Fig. 1. The surface area of HSAG increased with an increase of milling time due to the mechanical exfoliation and fragmentation of NG and xGnP. For first 300 min milling with SS balls, the NG showed more rapid increase of its surface area than xGnP. After 300min, the surface area of both NG and xGnP reached a plateau at about  $520$  and  $480\text{m}^2/\text{g}$ , respectively, despite further extended milling. The hard SS balls are more effective to increase the surface area of graphite than soft PP balls.

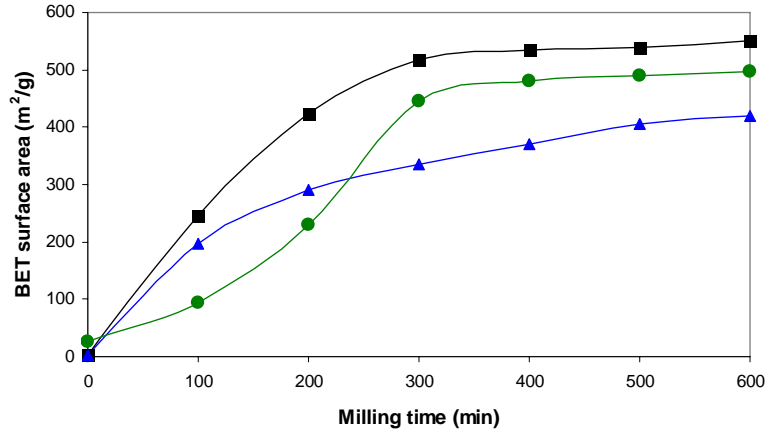


Figure 1. The BET surface area of milled graphites as a function of milling time: (■: HSANG with SS balls, ▲: HSANG with PP balls, ●: HSAGxGnP with SS balls).

Figure 2 shows the morphological changes in the process of mechanical milling of NG with SS and PP balls. The size-reduced thin graphite particles have typical platelet-type morphology (Fig. 2a), HSANG shows a smaller particle size but they are highly aggregated due to the pile-up of small particles onto relatively large ones and the high surface energy of the small particles (Fig. 2b~d). The particle agglomeration increases significantly as milling time increased. SS balls result in smaller particles and aggregates than the PP balls.

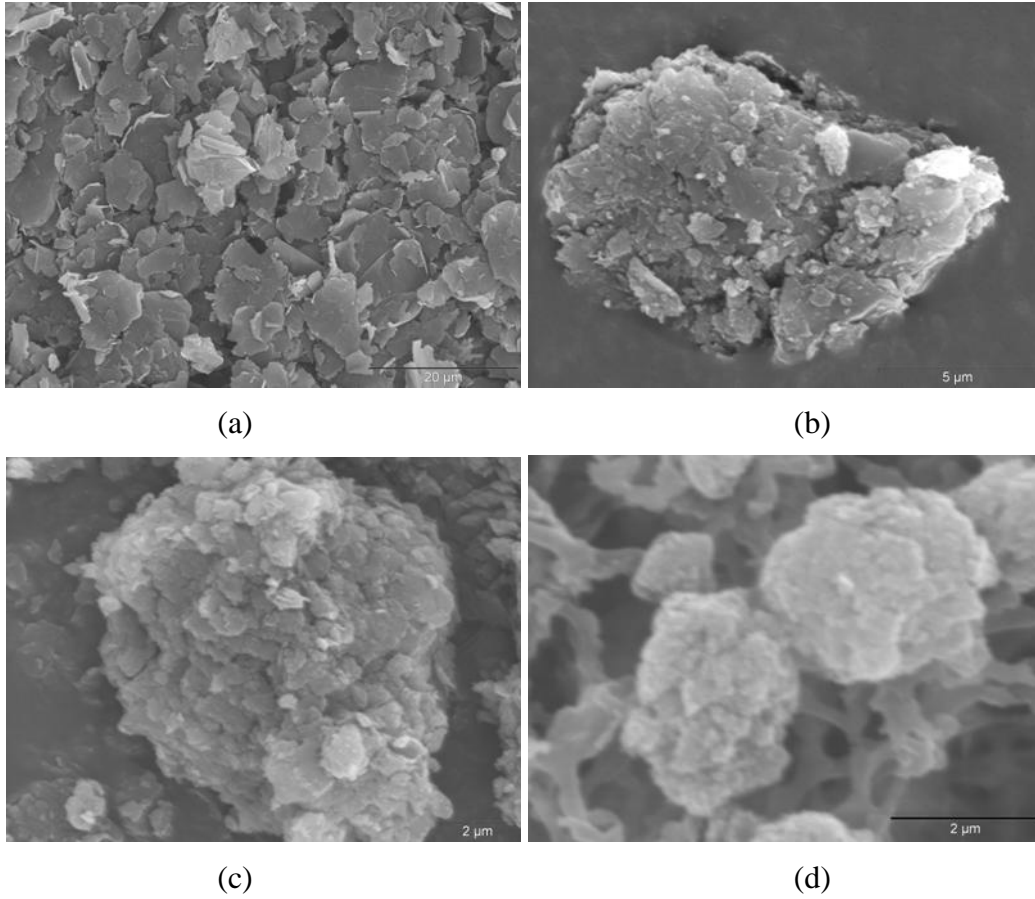
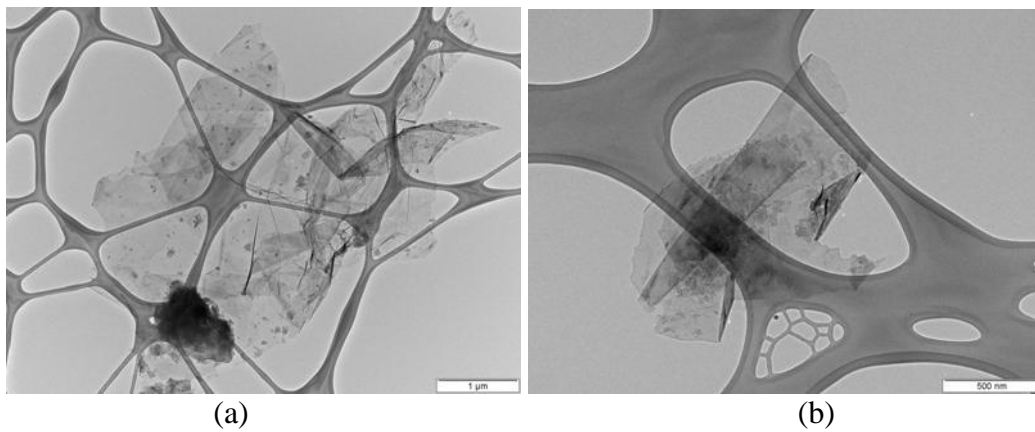


Figure 2. SEM images of (a) size-reduced thin graphite nanoparticle, (b) HSANG-250 with PP balls, (c) HSANG-400 with PP balls, (d) HSANG-400 with SS balls.

More detailed morphology of HSANG was observed by TEM. HSANG produced with soft PP balls retained its platelet morphology regardless of the milling time (Fig. 3a,b) and many particle fragments were found on the HSANG surface. However, HSANG made with SS balls showed a fractured and deformed morphology due to the higher energy input resulting in breakage of the covalent carbon-carbon bonds on the graphene basal plane by the desnerSS balls.



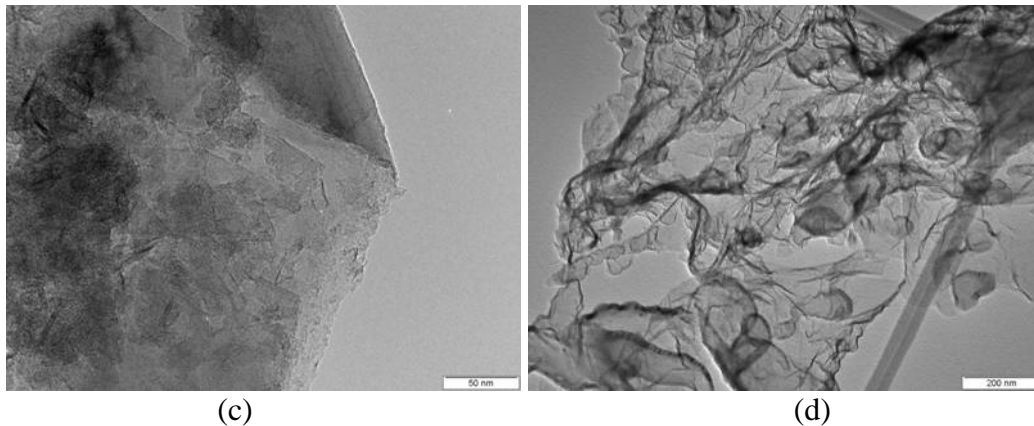


Figure 3. TEM images of (a) HSANG-250 and (b, c) HSANG-400 by using PP balls and HSANG-400 by using SS balls.

Figure 4 illustrates the thermal stability of HSANG fabricated by milling NG with SS balls and PP balls. The decomposition temperature decreased with increased milling time for both cases due to the reduction of size and thickness and the disruption of the graphene structure as a result of milling process. For HSANG with similar specific surface area (400min for PP ball and 200min for SS ball), SS balls caused more rapid mass loss at lower temperature than PP balls, implying that the hard balls create more defects in the graphite particles.

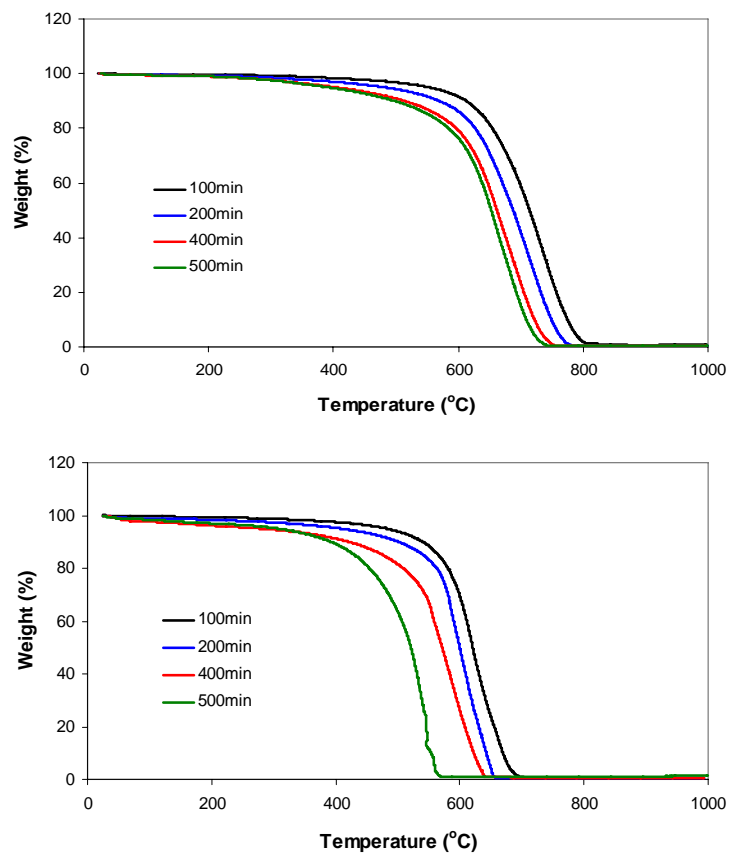


Figure 4. TGA behaviors of HSANG obtained with (top) PP balls and (bottom) SS balls.

The XRD patterns of HSANG milled with SS and PP balls for 100, 200, and 400 min are shown in Figure 5. A sharp decrease in intensity of peaks near  $26^\circ$  corresponding (002) crystalline structure of graphite is observed along with the increase of milling time. The peak of HSANG produced by milling over 400min with SS balls disappears. HSANG milled with SS balls showed more rapid decrease in intensity due to the creation of thin graphite as well as the creation of more defects and fragments which is consistent with TGA results.

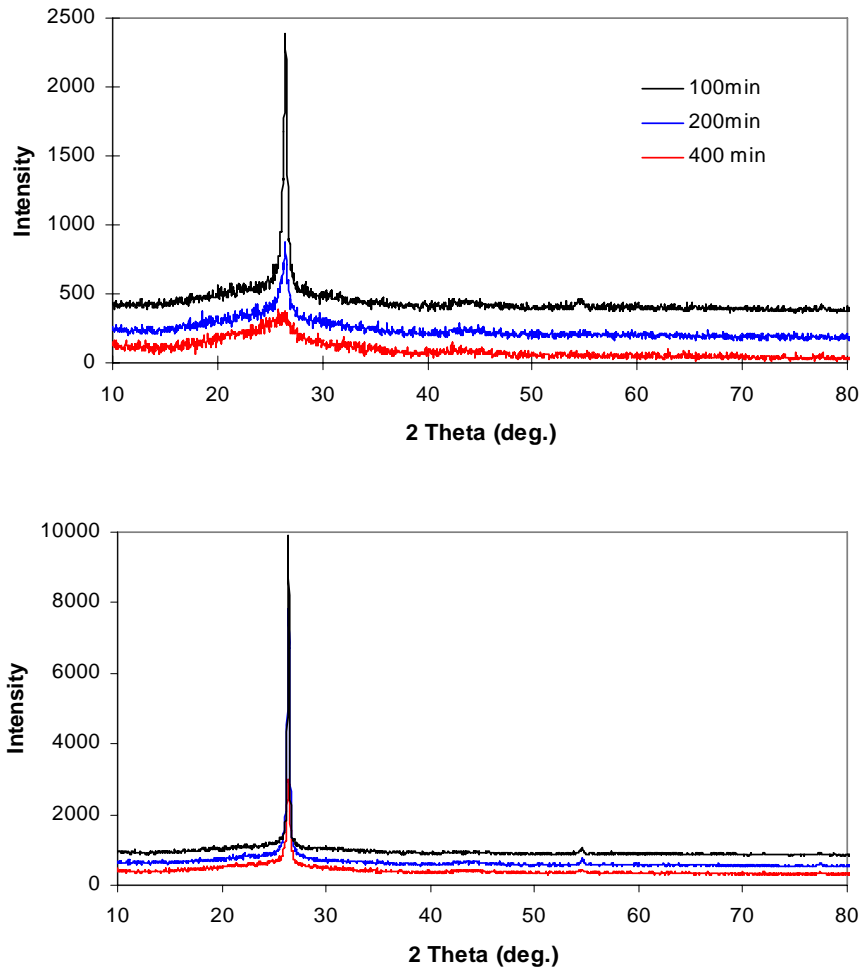


Figure 5. XRD patterns of NG milled with SS balls (top) and PP balls (bottom).

### Nanocomposite Properties

The effect of HSANG surface area on the flexural properties of 1wt.% of HSANG-reinforced VE nanocomposites is shown in Figure 6. The flexural modulus increased with HSANG addition, which is typical for inorganic filler-reinforced polymeric composites. The higher surface area HSANG is more effective in increasing the composite modulus. The flexural strength of the nanocomposites decreased with the HSANG addition. The poor dispersion of HSANG particles in matrix VE resin and the lack of HSANG-VE interaction may result in the reduction of flexural strength, as observed in the strength drop of HSANG-400 reinforced sample.

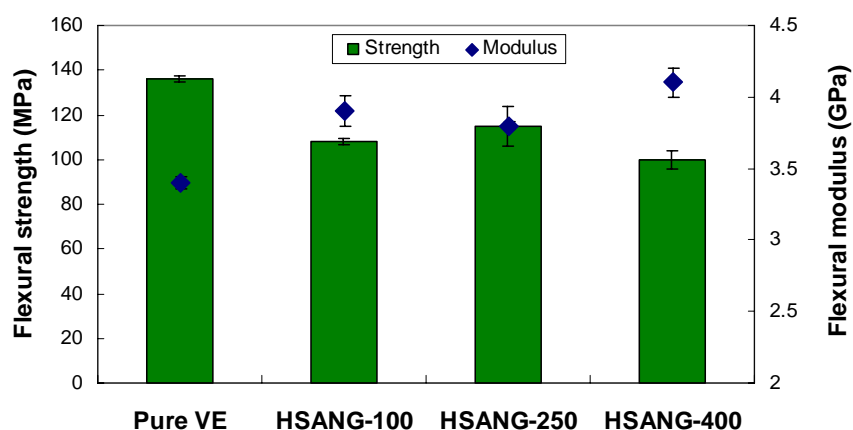


Figure 6. The flexural properties of VE composites reinforced with HSAG.

The flexural properties of VE nanocomposites reinforced with various graphites are shown in Figure 7. Similar to above case, the flexural strength decreased but the flexural modulus increased with the addition. The highest improvement of flexural modulus and the lowest strength were obtained from xGnP-15 because xGnP-15 has the highest aspect ratio and the lowest density of oxygen containing groups, which is confirmed by XPS analysis.

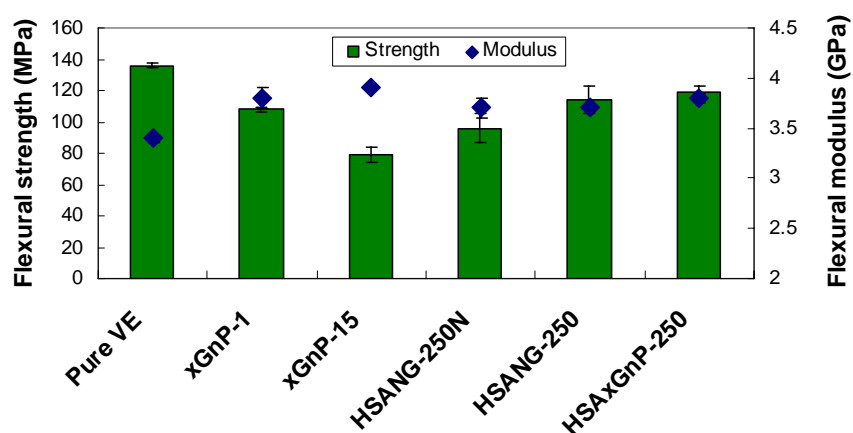


Figure 7. Flexural properties of VE composites reinforced with 1wt.% graphite.

The impact strength is a reflection of the toughness of the nanocomposites. Hence, the notch Izod impact strength of VE nanocomposites reinforced with xGnP and HSAG was measured and compared in Figure 8. The reinforced nanocomposites showed lower impact strength than pure vinyl ester due to the lack of sufficient graphite-vinyl ester interfacial interaction which plays an important role in an effective stress transfer and thus improvement of the composite toughness [11]. HSANG and HSAGxGnP had better impact strength than low surface area xGnP-1 and xGnP-15 due to the high density of oxygen groups on HSAG over xGnP but overall were not better than the neat vinyl ester matrix.

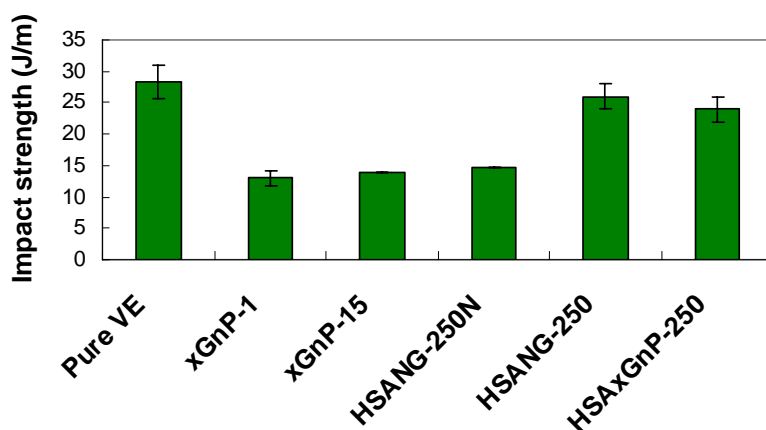


Figure 9. Impact strength of VE composites reinforced with 1wt.% graphite.

The electrical resistivity of the reinforced VE nanocomposites was also evaluated. As shown in Figure 10, high surface area graphite (HSANG and HSAXGnP) showed lower resistivity than either of the low surface area xGnP-1 and xGnP-15. However, the improvement of the composite conductivity was less than expected, which may be due to poor dispersion of agglomerated HSAG into VE matrix. Hence, it is a key challenge to enhance the dispersion of HSAG as well as other nano-reinforcing fillers throughout the polymeric matrix by modification of its surface chemistry to achieve a low percolation threshold.

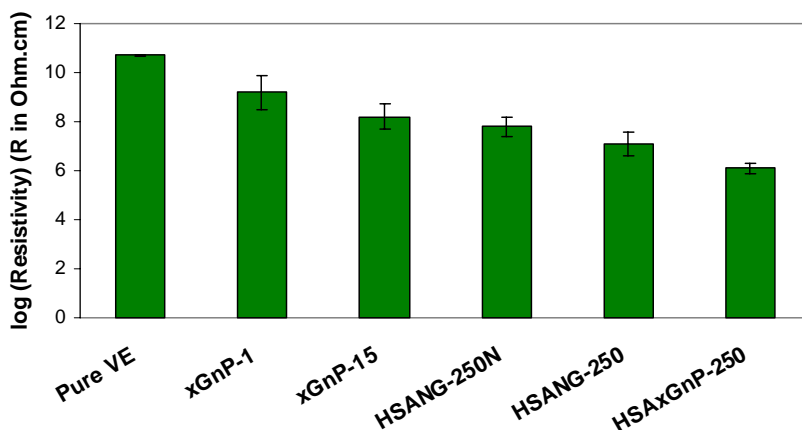


Figure 10. Electrical resistivity of VE nanocomposites reinforced with 1wt.% graphite.

## CONCLUSIONS

High energy milling process offers a direct mechanical method to reduce the size of graphites and increase their surface area. The produced HSAG can be good reinforcing filler for polymeric composites. HSAG-reinforced vinyl ester composites showed some improvement in both mechanical and electrical properties. It is expected that the utilization of HSAG as catalyst supports, absorbents, electrode materials, and fillers



strongly depends on the modification of the HSAG surface chemistry to improve its dispersion in liquids and polymeric matrices.

## References

1. J. Zhu, *Nature Nanotech.*, 2008, 3, 528-529.
2. M.D. Stoller, S. Park, Y. Zhu, R.S. Ruoff, *Nano Lett*, 2008, 8 (10), 3489-3502.
3. J. Lu, I.H. Do, L.T. Drzal, R.M. Worden, I. Lee, *ACS Nano*, 2008, 2(9), 1825-1832
4. E. Yoo, J. Kim, E. Hosono, H. Zhou, T. Kudo, I. Honma, *Nano Lett*, 2008, 8(8), 2277-2282.
5. A.K. Geim, K.S. Novoselov, *Nature Mater*, 2007, 6, 183-191.
6. L.T. Drzal; H. Fukushima, *U.S Pat. Appl. Publ.* 2004, 30pp.
7. W. Liu, I.H. Do, H. Fukushima, L.T. Drzal, 2007 Automotive Composites Conference Exhibition (ACCE), Sep. 11~13, Troy, MI.
8. R.Z. Sorensen, A. Klerke, U. Quaade, S. Jensen, O. Hansen, C.H. Christensen, *Catal. Lett*, 2006, 112, 77-81.
9. D.M. Nevskaya, E. Gastejales-Lopez, A. Guerrero-Ruiz, V. Munoz, *Carbon*, 2004, 42, 653-656.
10. M.R. Cuervo, E. Asedegbega-Nieto, E. Diaz, S. Ordonez, A. Vega, A.B. Dongil, I. Rodriguez-Ramos, *Carbon*, 2008, 46, 2096-2106.
11. K. Yang, M. Gu, Y. Guo, X. Pan, G. Mu, *Carbon*, 47, 1723-1737.